

# INVERSE BOUNDARY DESIGN PROBLEM OF COMBINED RADIATION CONVECTION HEAT TRANSFER IN A DUCT WITH DIFFUSE-SPECTRAL DESIGN SURFACE

Mohammad OMIDPANAHA<sup>a</sup>, Seyed Abdolreza GANDJALIKHAN NASSAB<sup>a 1</sup>

<sup>a</sup> - Department of Mechanical Engineering, School of Engineering, Shahid Bahonar University of Kerman, Kerman, Iran

*In the present work, an optimization technique is applied for inverse boundary design problem of radiative convective heat transfer of laminar duct flow by numerical method. The main goal is to verify how the solution of inverse problem is affected by the spectral behavior of the boundary surfaces. The conjugate gradient method is used to find the unknown temperature distribution over the heater surface to satisfy the prescribed temperature and heat flux distributions over the design surface. The bottom boundary surface (including design surface) is diffuse-spectral, while the top wall (heater surface) behaves as gray one. The variation of emissivity with respect to the wavelength is approximated by considering a set of spectral bands with constant emissivity and then the radiative transfer equation is solved by the discrete ordinates method for each band. The performance of the present method is evaluated by comparing the results with those obtained by considering a diffuse-gray design surface. Finally an attempt is made to investigate the spectral behavior of the design surface on the calculated temperature distribution over the heater surface.*

*Keywords: Convection, Radiation, Inverse Problem, Conjugate Gradient Method, Spectral surface*

## 1. Introduction

Combined convection and radiation heat transfer in an absorbing, emitting and scattering medium has a main role in many engineering applications such cooling of electronic systems, power generating equipment, gas turbine blades, heat exchangers and combustion chambers. It may be required that the temperature of a processing material inside a furnace be uniform to avoid thermal stresses and obtain high quality materials, which could

---

<sup>1</sup>Corresponding author; e-mail: [ganj110@uk.ac.ir](mailto:ganj110@uk.ac.ir)

be achieved only by providing a uniform heat flux distribution on the material. In such cases, inverse boundary design analysis could be employed to achieve two uniform boundary conditions (temperature and heat flux) over some parts of a system. One of the most well-known and powerful methods to solve the integro-differential radiative transfer equation (RTE) in a participating media is the discrete ordinates method (DOM) with its variations and improvements [1]. Chandrasekar in 1950 [2] formulated this technique at first, then this technique has been studied and improved by Carlson and Lathrop in 60-70's [3] and by Fiveland and Truelove in the 80's [4, 5].

In the field of combined conduction-radiation problems, Razzaque et al. [6] studied a conduction-radiation problem inside a two-dimensional rectangular geometry using the finite element method limited to only non-scattering participating medium with isothermal black walls. Tan [7] applied the product integration method to solve combined conduction-radiation problem in a square enclosure with isothermal walls. The discrete ordinates method used by Kim et al. [8] for combined radiative and conductive heat transfer in rectangular enclosures while Rouse et al. [9] employed the Control-Volume Finite Element Method (CVFEM) to solve combined mode of heat transfer in two-dimensional cavities. Talukdar et al. [10] employed the Collapse dimension method to study combined conduction-radiation problems. Mahapatra et al. [11] investigated a new hybrid method to analyze coupled conduction and radiation heat transfer in two-dimensional planar geometry. Recently, Amiri et al. [12] solved the problem of combined conduction and radiation heat transfer in 2D irregular geometries with anisotropic-scatter participating media, using DOM and blocked-off method.

A number of recent numerical research works in the field of radiation heat transfer have dealt with inverse design problems. For solving these types of boundary design problems, the use of regularization techniques often leads to a mathematically ill-posed problem, and special methods are required to treat this difficulty. Harutunian et al. [13] first applied the regularization techniques for analysis of a radiant enclosure with diffuse and gray walls. Howell et al. [14] obtained an approximate initial design set for using in the sophisticated available design tools by applying the regularization techniques. In several other studies, inverse methods were extended to boundary design of radiant enclosures containing participating media [15,16]. Franca et al. [17] extended this method to design radiant furnaces with considering other modes of heat transfer . Recently, optimization techniques have been employed to design thermal systems in which radiation is the dominant heat transfer. These works were on the basis of minimizing an objective function such that its minimum corresponds to the ideal design configuration. The optimization methods replace the ill-

conditioned problem with a well-posed **one** that must be solved repetitively through a systematic approach to an optimum solution. First, Fedrov et al. [18] used the optimization techniques for obtaining optimal radiant heater settings in an industrial oven. Optimum design of radiant enclosures containing a transparent medium was done by Daun et al. [19]. A new methodology was proposed by Sarvari et al. [20–22] for design of radiant enclosures containing absorbing–emitting media in order to distinguish the appropriate heater settings. Sarvari and Mansouri [23] used the optimization procedure to determine the heat source distribution in radiating media inside a thermal system. This procedure was extended by Sarvari [24] to find the heat source distribution in combined conductive radiative heat transfer inside a complex geometry enclosure.

In all mentioned research works, the radiant enclosures were considered with gray-diffuse boundary walls whose radiative properties (emissivity and absorptivity) did not depend on direction or wavelength. It is clear that in **many** practical cases, the radiative properties of surfaces depend on wavelength as well as temperature. These surfaces are called diffuse-spectral surfaces.

Recently, an optimization technique was employed to inverse design of radiative furnaces with diffuse-spectral surfaces by Bayat et al. [25]. In that work, the design surface was considered to be spectral such that the variation of its emissivity with respect to the wavelength was approximated by a set of spectral bands with constant emissivities and then the RTE was solved by the net radiation method considering transparent medium for each band. The temperature distribution over the heater **surface** was estimated by employing the well-known conjugate gradient method. It was found that the heater temperature distribution is much affected **by the spectral behavior of design surface.**

Study of literature shows that, the inverse boundary design technique has not been employed in combined convection-radiation heat transfer with the presence of diffuse-spectral design surface. This problem can show how the solution of inverse design is affected by the variation of radiant properties of design surface with wave number. Also, an attempt is made to compare the solutions of inverse problem with gray and spectral design surfaces. The fluid is considered to be a homogenous gray absorbing-emitting-scattering medium. All thermo-physical properties are assumed to be constant. The duct's upper wall (heater surface) is

considered to be gray while the duct's bottom wall (including design surface) behaves as diffuse-spectral. An optimization technique based on the conjugate gradient method is applied to minimize an objective function which is defined as sum of square errors between the exact and estimated heat fluxes over the design surface. The finite difference method is used to solve energy equation with radiation and convection terms. For the spectral design surface, the variation of emissivity with respect to the wavelength is approximated by considering a set of spectral bands with constant emissivities and then the radiative transfer equation is solved at each band. The discrete ordinate method is applied to solve radiative transfer equation, which is discretized by the FVM. The radiative convective model is validated along a direct problem by comparison with the well-documented results reported by other investigators.

## 2. Problem description

Figure 1 shows a schematic view of the two-dimensional rectangular duct with length  $L$ , in which laminar convection flow of radiating gray gas takes place. The heater surface is located on the top wall with length  $L$ . The design surface is located in the center of the bottom wall with length  $2L/3$ . The design surface and bottom wall temperatures are at  $T_w$ . The duct's upper wall has constant emissivity equal to  $\varepsilon_w$ , while the design surface emissivity is a function of wave length. It is desired to find the unknown temperature profile over the heater surface to satisfy uniform temperature of  $T_D$  and constant heat flux equal to  $Q_D$  over the design surface.

## 3. Direct problem

The energy equation for steady laminar convection flow of radiating gas with absorbing, emitting and scattering abilities is as follows:

$$\rho c_p \left( u \frac{\partial T}{\partial X} + v \frac{\partial T}{\partial Y} \right) = k \left( \frac{\partial^2 T}{\partial X^2} + \frac{\partial^2 T}{\partial Y^2} \right) - \nabla \cdot \mathbf{Q}_r \quad (1)$$

In the present study, the laminar duct flow is considered to be fully developed with parabolic velocity profile. To obtain the temperature distribution inside the convective flow by solving Eq. (1), it is necessary to relate  $\nabla \cdot \mathbf{Q}_r$  to the temperature distribution within the

participating medium. One approach is to obtain  $\nabla \cdot Q_r$  directly by considering the local radiative interaction with a differential volume in the medium. The local divergence of the radiative flux is related to the local intensities by:

$$\nabla \cdot Q_r = \sigma_a [4\pi I_b(r) - G(r)] \quad (2)$$

Where  $G(r)$  is incident radiation,

$$G(r) = \int_{4\pi} I(r, \Omega) d\Omega \quad (3)$$

For calculation of radiation intensity field and  $\nabla \cdot Q_r$ , it is necessary to solve the radiative transfer equation. Since the design surface is a spectral one whose emissivity depends on the wave number, the RTE should be written and solved for each wave number. The spectral form of this equation for an absorbing, emitting and scattering gray medium can be written as in Modest [26],

$$\vec{s} \cdot \nabla I_\lambda(\vec{r}, \vec{s}) = \sigma_a(\vec{r}) I_{b\lambda}(\vec{r}) - (\sigma_a + \sigma_s) I_\lambda(\vec{r}, \vec{s}) + \frac{\sigma_s(\vec{r})}{4\pi} \int_{4\pi} I_\lambda(\vec{r}, \vec{s}') \phi(\vec{r}, \vec{s}, \vec{s}') d\Omega' \quad (4)$$

where  $I_\lambda(\vec{r}, \vec{s})$  is the radiation intensity per unit wave length in position  $\vec{r}$ , and in the direction  $\vec{s}$ ,  $I_{b\lambda}(\vec{r})$  is the black body radiation intensity per unit wave length in the position  $\vec{r}$  and at the temperature of medium,  $\sigma_a$  and  $\sigma_s$  are the gray medium absorption and scattering coefficients, respectively,  $\beta = (\sigma_a + \sigma_s)$  is the extinction coefficient, and  $\phi(\vec{r}, \vec{s}, \vec{s}')$  is the scattering phase function which is considered to be unity because of the isotropic scattering in all of the case studies.

For spectral and diffuse reflecting surfaces, the radiative boundary condition for Eq. (4) is:

$$I_{w,\lambda} = \varepsilon_{w,\lambda} I_{b\lambda}(\vec{r}) + \frac{(1 - \varepsilon_{w,\lambda})}{\pi} \int_{\hat{n} \cdot \vec{s}' < 0} I_\lambda(r_w, s') |\hat{n} \cdot \vec{s}'| d\Omega' \quad (5)$$

Where  $\vec{r}$  belongs to the boundary surface and Eq. (5) applies for  $\hat{n} \cdot \vec{s} \geq 0$ ,  $I_{w,\lambda}(r_w, s)$  is the radiation intensity leaving the surface,  $\varepsilon_{w,\lambda}$  is the surface spectral emissivity and  $\hat{n}$  is the unit vector normal to the boundary surface. As mentioned before, the RTE should be solved at each band where the design surface has constant emissivity and behaves as gray wall. Considering this fact, the value of  $I_{b\lambda}$  in Eq. (5) is calculated as follows:

$$I_{b\lambda} = \Delta F I_b = \Delta F \frac{\sigma T^4}{\pi} \quad (6)$$

Where

$$\Delta F = F(0 \rightarrow \lambda_2 T) - F(0 \rightarrow \lambda_1 T) \quad (7)$$

$$F(0 \rightarrow \lambda_1 T) \equiv \frac{\int_0^{\lambda_1} e_{b\lambda} d\lambda}{\int_0^{\infty} e_{b\lambda} d\lambda} \quad (8)$$

Which is calculated based on the following series [27]:

$$F(0 \rightarrow \lambda T) = \frac{15}{\pi^4} \sum_{n=1}^{\infty} \frac{e^{-nv}}{n} \left( v^3 + \frac{3v^2}{n} + \frac{6v}{n^2} + \frac{6}{n^3} \right) \quad (9)$$

In the above equations,  $e_{b\lambda}$  is the Planck's blackbody function,  $v = \frac{C_2}{\lambda T}$  and  $C_2 = 14388 \mu\text{mk}$ . By this technique, the RTE can be solved for obtaining the spectral radiant intensity distribution inside the participating media. An example of band division for germanium with spectral data at 333 K are given in Table 1.

The radiative transfer equation is an integro-differential equation that can be solved using the discrete ordinates method. In the DOM, Eq. (4) is solved for a set of  $n$  different directions,  $\vec{s}_i$ ,  $i=1,2,3,\dots,n$  and integrals over solid angle are substituted by the numerical quadrature, that is,

$$\int_{4\pi} f(\vec{s}) d\Omega \cong \sum_{i=1}^n w_i f(\vec{s}_i) \quad (10-a)$$

where  $w_i$  are the quadrature weights associated with the directions  $\vec{s}_i$ .

According to this method, RTE is approximated by a set of  $n$  equations, as follows [26]:

$$(\vec{s}_i \cdot \nabla) I_{\lambda}(\vec{r}, \vec{s}_i) = \sigma_a I_{b\lambda}(\vec{r}) - (\sigma_a + \sigma_s) I_{\lambda}(\vec{r}, \vec{s}_i) + \frac{\sigma_s}{4\pi} \sum_{j=1}^n I_{\lambda}(\vec{r}, \vec{s}_j) \phi(\vec{s}_j, \vec{s}_i) w_j \quad i=1,2,3,\dots,n \quad (10-b)$$

subjected to the boundary conditions:

$$I_g(\vec{r}_w, \vec{s}_i) = \varepsilon_w I_b(\vec{r}_w) + \frac{(1 - \varepsilon_w)}{\pi} \sum_{\vec{n}_w \cdot \vec{s}_j < 0} I_g(\vec{r}_w, \vec{s}_j) |\vec{n}_w \cdot \vec{s}_j| w_j \quad \vec{n}_w \cdot \vec{s}_i > 0 \quad (10-c)$$

More details of the numerical solution of RTE by DOM coupled with energy equation in convection flow of radiating gas was described in the previous paper by the second author [28].

Accordingly, the value of incident radiation  $G$  at each computational grid is obtained as follows:

$$G = \sum_{k=1}^{N_k} \sum_{m=1}^{N_m} w_k I_{p,k}^m \quad (10-d)$$

Which is needed for computation of radiative term in the right hand side of energy equation. In the above equation,  $N_k$  is the number of directions and  $N_m$  is the number of bonds at which RTE is solved. Besides, radiant heat flux distribution over the boundary walls can be obtained as follows:

$$Q_r = \sum_{m=1}^{N_m} \pi (\varepsilon_{w\lambda} I_{b\lambda}(\vec{r}) - \frac{\varepsilon_{w\lambda}}{\pi} \sum_{\hat{n} \cdot \hat{s} < 0}^{N_k} I_{\lambda} |\hat{n} \cdot \hat{s}| d\Omega) \quad (11)$$

The convective heat flux over the boundary wall is defined as:

$$Q_c = -k \frac{\partial T_w}{\partial Y} \quad (12)$$

And the total heat flux is computed by:

$$Q_T = Q_c + Q_R \quad (13)$$

Since in the present study, a comparison is made between the solutions of inverse problem for spectral and gray design surfaces, the value of equivalent gray surface emissivity for the design surface is evaluated as follows [27]:

$$\varepsilon(T) = \frac{1}{E_b(T)} \int_0^{\infty} \varepsilon(\lambda, T) e_{b\lambda}(\lambda, T) d\lambda \cong \sum_{m=1}^M \varepsilon_m \Delta F_m(T) \quad (14)$$

#### 4. Inverse problem

the present inverse problem, the conjugate gradient method is applied to estimate the unknown temperature distribution,  $T_h(X)$  over the heater surface. Inverse boundary design problems usually require two boundary conditions over a desired surface (design surface) to estimate unspecified boundary condition over some parts of a system (heater surface). These two boundary conditions can be (temperature, heat flux, incident radiation, etc.) measured by special methods and instruments, which used as extra data to solve the inverse problem. In the present inverse problem, temperature and heat flux distributions over the design surface are applied to solve the inverse problem. The conjugate gradient method is a powerful technique based on minimizes an objective function,  $G$ , which is calculated as the sum of square errors between estimated and desired heat fluxes on the design surface as follows [29]:

$$G = \sum_{n=1}^N (Q_{d,n} - Q_{e,n})^2 \quad (15)$$

In Eq. (15),  $Q_e$  and  $Q_d$  are the estimated and desired heat fluxes along the design surface, respectively. Besides,  $N$  is the number of nodes and  $n$  the node number on design surface. The heater surface temperature at iteration  $k + 1$  is updated as follows:

$$T_{h,m}^{k+1} = T_{h,m}^k - \psi^k d_m^k \quad (16)$$

Where  $\psi^k$  is the search step size at  $k$  level of iteration procedure and  $d^k$  is direction of descent given by:

$$d_m^k = \nabla G_m^k + \gamma^k d_m^{k-1} \quad (17)$$

In Eq. (17)  $\gamma$  is the conjugate coefficient which is stated as below:

$$\gamma^k = \frac{\sum_{m=1}^M [(\nabla G_m^k)(\nabla G_m^k - \nabla G_m^{k-1})]}{\sum_{m=1}^M (\nabla G_m^{k-1})^2} \quad \text{with } \gamma^0 = 0 \quad \text{when } k = 0 \quad (18)$$

To obtain  $\nabla G$ , Eq. (15) must be differentiated with respect to unknown parameter  $T_{h,m}$ . Thus:

$$\nabla G_m^k = -2 \sum_{n=1}^N J_{nm}^k (Q_{d,n} - Q_{e,n}^k) \quad (19)$$

Here,  $J_{nm}^k = \frac{\partial Q_{e,n}^k}{\partial T_{h,m}^k}$  is the sensitivity coefficient that can be obtained by numerical solution of

sensitivity problem. Finally the search step size can be defined as:

$$\psi^k = \frac{\sum_{m=1}^M \sum_{n=1}^N (J_{nm}^k d_m^k)(Q_{e,n}^k - Q_{d,n})}{\sum_{m=1}^M \sum_{n=1}^N (J_{nm}^k d_m^k)(J_{nm}^k d_m^k)} \quad (20)$$

Numerical technique in solving the sensitivity problem was given in the previous work by the second author [30], and is not explained here for space saving.

## 5. Strategy of numerical computations

The present inverse problem is solved with conjugate gradient method by applying the following algorithm. An initial guess is considered for the unknown temperature distribution over the heater surface,  $T_h^0(X)$ , and then the following steps are performed:



Step1. The temperature field in the radiating medium is obtained via the direct problem.

Step2. The objective function  $G$  is calculated by Eq. (15) and if it is smaller than a pre-specified value, the procedure is terminated, otherwise the next step should be done.

Step3. By the temperature field inside the medium from step 1, the sensitivity problem is solved.

Step4. The values of direction of descant, conjugation coefficient, gradient direction and search step size are calculated by Eqs. 17, 18, 19 and 20, respectively.

Step 5. The new estimation for  $T_h^{k+1}(X)$  is achieved and computation is repeated from step 1.

Since the conjugate gradient method is a time-consuming process particularly in the cases of having large number of parameters to be estimated, it is necessary to work with optimum grid size to reduce computational time and for obtaining grid independent solution. Based on the grid independent study, the optimized mesh size  $60 \times 20 (N_x \times N_y)$  is distinguished such that all of the subsequent calculations are drawn with this discretized computational domain.

## 6 .Validation

First to demonstrate the trend of convergency in the present computation, the values of objective function for both spectral design surfaces at each iteration level are drawn in Fig. 2. The computational times are also mentioned in this figure. As seen, the amount of error has decreasing trend along the iterative calculation, such that for Germanium whose spectral emissivity is greater than the one for Silicon, more iteration levels is needed to reach the converged solution.

To verify the accuracy of the inverse problem, we use the results of previous problem in mesh study for combined radiation convection heat transfer in duct flow. After insuring verification of the direct problem, total heat flux distribution over the design surface (a part of the bottom wall) is considered as additional information for an inverse problem. In inverse problem, the duct upper wall is considered to be the heater surface. Now, the problem is to find the unknown temperature distribution over the heater surface, to obtain both uniform temperature and prescribed heat flux distributions over the design surface. As we expect, the

heater must have a uniform temperature distribution all over its surface. Fig. 3 shows the comparison of estimated and the exact temperature distribution over the heater surface. As seen, the estimated temperature has an acceptable deviation with the exact one.

## 7. Results

The inverse problem of 2-*D* laminar convection flow of radiating gases through a rectangular duct with both gray and spectral boundary walls is considered in the present work. The duct's upper wall has constant emissivity, while the emissivity of bottom surface (including design surface) is a function of wave length. The design surface is under both uniform temperature and heat flux. The values of parameter which are used in the numerical simulations are given in Table 2. In all incoming computations, the temperature distribution over the heater surface is the unknown variable that must be determined via the inverse problem. The purpose is to study the effect of spectral behavior of design surface on the solution of inverse problem. Besides, an attempt is made to compare the solutions obtained for spectral design surface with equivalent gray one whose emissivity is calculated by Eq. (14). In the present work, two different spectral design surfaces made by Silicon and Germanium are considered whose emissivities at two different constant temperatures depend on wave length as shown in Fig. 4. These special two materials are selected because, the emissivity of Silicon depends strongly on wave length compared to temperature and opposite behavior is seen for the Germanium.

First, to show the thermal behavior of convective flow, the temperature field inside the participating medium is presented in Fig. 5. This figure depicts high temperature region near to the heater surface, especially at the entrance region. As the flow passes through the channel, its temperature increases because of the radiative and convective heat transfer from the heater hot surface. Besides, closed to the bottom wall, the fluid temperature is almost uniform because of the isothermal design surface which is kept at a constant desired temperature.

The temperature distributions over the heater surface for two different spectral design surfaces made by Silicon and Germanium and also for their equivalent gray surfaces are drawn in Fig. 6. This figure reveals that for both spectral and gray cases, higher temperature over the heater surface is needed for the Germanium. This is due to this fact that at the considered design surface, i.e.  $T_D = 333\text{ K}$ , the spectral emissivity of Germanium is much

lower **than** that is for Silicon, such that it needs more radiant outgoing heat flux from the heater surface for achieving constant temperature of  $T_D = 333\text{ K}$ . Besides, Fig. 6 demonstrates that for both Silicon and Germanium, the temperature of heater surface increases due to spectral behavior of the design surfaces, such that this is much more for the Silicon that has higher rate of emissivity variation with the wave number. The spectral effect of design surface on the convective and radiative heat flux distributions over the heater surface is studied in Fig. 7. As seen from Fig. 7-a, there is not considerable difference between the gray and spectral cases, especially for the convective heat flux distribution at downstream region of the heater surface, such that the maximum rate of convective heat flux is needed for the Germanium with spectral behavior. But Fig.7-b shows that spectral behavior of design surface has more effect of heater radiative heat flux, and the highest rate of radiative heat flux is for the case using Germanium whose emissivity depends on the wavelength.

The distributions of relative error ( $E_{rel}$ ) of the estimated heat flux over the design surfaces made by Germanium and Silicon for both spectral and their equivalent gray behavior are presented in Fig. 8. The relative error is defined as:

$$E_{rel} = \frac{(Q_{d,n} - Q_{e,n})}{|Q_{d,n}|} \times 100 \quad (21)$$

Where  $Q_e$  and  $Q_d$  are the estimated and desired heat fluxes along the design surface. As seen for all of the cases, the maximum value of relative error is about 0.3% that happens on the upstream region of the design surface, and on other parts, the relative error decreases so much that leads to having average relative error less than 0.05% over the whole part of the design surface. Besides, Fig. 8 reveals that the value of relative error is not much affected by the spectral behavior of design surfaces for both Germanium and Silicon materials.

As it was mentioned before, the present calculations include both temperatures of 333K and 433K for the design surface. To study more about the effect of spectral behavior of design surface on the solution of inverse boundary design problems, the temperature distribution over the heater surface at  $T_D = 433\text{ K}$  is calculated and plotted in Fig. 9. This figure reveals that the spectral behavior of Silicon has great effect on the temperature of heater surface and causes considerable increase on the value of this parameter. But for Germanium, whose emissivity does not depend strongly on the wave number, the heater surface temperature for the spectral and equivalent gray cases are very closed to each other. Besides, Fig. 9 shows that at  $T_D = 433\text{ K}$ , the heater surface needs lower temperature for the

Germanium in comparison to the Silicon which is in opposite to findings at  $T_D = 333$  K (Fig. 6). This is due to this fact that at 433K, the Germanium has high emissivity that needs less outgoing radiative heat flux from the heater surface.

## 8. Conclusions

The present work describes the inverse boundary design in a convection flow of radiating gas in a duct where the temperature distribution on the heater surface was determined to satisfy the specified temperature and heat flux distributions along the design surface. The spectral behavior of the design surface on the solution of inverse problem was emphasized in this numerical study. The Germanium and Silicon as two spectral design surfaces were considered in the computations. The theoretical formulation was explained by a set of high non-linear equations govern to a combined convection-radiation heat transfer in duct flow. The DOM was employed to solve the RTE, while the energy equation was numerically solved by the finite volume technique. Besides, the conjugate gradient method was used to find the unknown temperature distribution over the heater surface. Numerical results showed that the solution of inverse problem is affected by the spectral behavior of the design surfaces, such that in all of the test cases, the temperature over the heater surface increases due to dependence of design surface emissivity with the wave number.

## NOMENCLATURE

$d$	direction of descent
$E$	error
$G$	objective function
$H$	height of the channel, [m]
$I$	radiation intensity, [W/ m <sup>2</sup> ]
$J$	sensitivity matrix
$k$	thermal conductivity, [W / mK]

$L$	length of the duct, [m]
$M$	number of nodes on heater surface
$N$	number of nodes on design surface
$Q$	heat flux, [W/ m <sup>2</sup> ]
$T$	temperature, [K]
$w$	quadrature weight associated with the direction $s$
$X, Y$	dimensional coordinates, [m]

### **Greek Symbols**

$\beta$	extinction coefficient, [1/ m]
$\delta$	Dirac delta function
$\varepsilon$	wall emissivity
$\phi$	scattering phase function, inclination angle
$\gamma$	conjugate coefficient
$\eta$	derivation of radiation intensity with respect to the heater element
$\lambda$	wave number
$\sigma$	Stefan Boltzman's constant = $5.67 \times 10^{-8}$ [W / m <sup>2</sup> K <sup>4</sup> ]
$\sigma_a$	absorption coefficient, [1/ m]
$\sigma_s$	scattering coefficient, [1/ m]
$\omega$	scattering albedo
$\psi$	search step size

$\zeta$  derivation of temperature with respect to the heater element

### Subscripts

$B$  bottom

$d, D$  design surface, desired heat flux

$h, H$  heater surface

$k$  iteration number

$L$  left

$m$  node number on heater surface

$n$  node number on design surface

$r, R$  radiation, right

$rel$  relative

$rms$  root mean square

$R$  radiative

$T$  total heat flux

$w$  wall

### References

[1] Rouse, D. R., Numerical predictions of two-dimensional conduction, convection, and radiation heat transfer— I. Formulation, *International Journal of Thermal Sciences*, 39 (2000), pp. 315-331

[2] Chandrasekhar, S., *Radiative transfer*, Clarendon Press, Oxford, 1950

[3] Carlson, B. G., Lathrop, K. D., *Transport theory—the method of discrete ordinates in: Computing methods of reactor physics*, Gordon & Breach, New York, 1968

[4] Fiveland, W.A., Discrete-ordinates solutions of the radiative transport equation for rectangular enclosures, *Journal of Heat Transfer*, 106 (1984), 4, pp.699-706

- [5] Truelove, J. S., Three-dimensional radiation in absorbing-emitting-scattering in using the discrete ordinates approximation, *Journal of Quantitative Spectroscopy & Radiative Transfer*, 39 (1998), pp. 27-31
- [6] Razzaque, M. M., Howell, J. R., Klein, D. E., Coupled radiative and conductive heat transfer in a two dimensional rectangular with gray participating media using finite elements, *Journal of Heat Transfer*, 106 ( 1984), pp. 613-619
- [7] Tan, Z., Combined radiative and conductive transfer in two-dimensional emitting, absorbing, and anisotropic scattering square media, *International Communications in Heat and Mass Transfer*, 16 (1989), pp. 391-401
- [8] Kim, T. Y., Baek, S. W., Analysis of combined conductive and radiative heat transfer in a two dimensional rectangular enclosure using the discrete ordinates method, *International Journal of Heat and Mass Transfer*, 34 (1991), pp. 2265-2273
- [9] Rouse, D. R., Gautier, G., Sacadura, J. F., Numerical predictions of two-dimensional conduction, convection and radiation heat transfer – II. Validation, *International Journal of Thermal Sciences*, 39 ( 2000), pp. 332-353
- [10] Talukdar, P., Mishra, S. C., Transient conduction and radiation heat transfer with heat generation in a participating medium using the collapsed dimension method, *Numerical Heat Transfer—Part A*, 39 (2001), pp. 79-100
- [11] Mahapatra, S. K., Nanda, P., Sarkar, A., Analysis of coupled conduction and radiation heat transfer in presence of participating medium using a hybrid method, *Heat Mass Transfer*, 41 (2005), pp. 890-898
- [12] Amiri, H., Mansouri, S. H., Safavinejad, A., Combined conductive and radiative heat transfer in an anisotropic scattering participating medium with irregular geometries, *International Journal of Thermal Sciences*, 49(2010), pp. 492-503
- [13] Harutunian, V., Morales, J. C., Howell, J. R., Radiation exchange within an enclosure of diffuse-gray surfaces: the inverse problem (No. CONF-950828), *American Society of Mechanical Engineers*, New York, NY (United States)
- [14] Howell, J., Ezekoye, O., Morales, J., Inverse design model for radiative heat transfer, *Journal of heat transfer*, 122 (2000), 3, pp. 492-502
- [15] Morales, J. C., Harutunian, V., Oguma, M., Howell, J. R., Inverse design of radiating enclosures with an isothermal participating medium, ICHMT Digital Library Online: Begel House Inc., (1995),  
<http://www.dl.begellhouse.com/references/1bb331655c289a0a,63045c9947e5cdf6,6d79ace923db0293.html>
- [16] Franca, F., Morales, J.C., Oguma, M., Howell, J.R., Inverse radiation heat transfer within enclosures with non isothermal participating media, *In Heat Transfer Conference*, (1998), Vol. 7, pp. 433-438
- [17] Franca, F. H., Ezekoye, O. A., Howell, J. R., Inverse boundary design combining radiation and convection heat transfer, *ASME Journal of heat transfer*, 123 (2001), 5, pp. 884-891
- [18] Fedorov, A. G., Lee, K. H., Viskanta, R., Inverse optimal design of the radiant heating in materials processing and manufacturing, *Journal of Materials Engineering and Performance*, 7 (1998), 6, pp. 719-726
- [19] Daun, K. J., Howell, J. R., Morton, D. P., Design of radiant enclosures using inverse and non-linear programming techniques, *Inverse Problems in Engng.*, 11 (2003), 6, pp. 541-560
- [20] Hosseini Sarvari, S. M., Mansouri, S. H., Howell, J. R., Inverse boundary design radiation problem in absorbing-emitting media with irregular geometry, *Numerical Heat Transfer: Part A: Applications*, 43 (2003), 6, pp. 565-584

- [21] Sarvari, S. H., Mansouri, S. H., Howell, J. R., Inverse Design of Three Dimensional Enclosures with Transparent and Absorbing-Emitting Media using an Optimization Technique, *International communications in heat and mass transfer*, 30 (2003), 2, pp. 149-162
- [22] Hosseini Sarvari, S. M., Howell, J. R., Mansouri, S. H., Inverse boundary conduction-radiation problem in irregular two-dimensional domains, *Numerical Heat Transfer: Part B: Fundamentals*, 44 (2003), 3, pp.209-224
- [23] Sarvari, S. H., Mansouri, S. H., Inverse design for radiative heat source in two-dimensional participating media, *Numerical Heat Transfer, Part B*, 46 (2004), 3, pp. 283-300
- [24] Sarvari, S. H., Inverse determination of heat source distribution in conductive-radiative media with irregular geometry, *Journal of Quantitative Spectroscopy and Radiative Transfer*, 93 (2005), 1, pp. 383-395
- [25] Bayat, N., Mehraban, S., Sarvari, S. H., Inverse boundary design of a radiant furnace with diffuse-spectral design surface, *International Communications in Heat and Mass Transfer*, 37 (2010), 1, pp. 103-110
- [26] Modest, M. F., *Radiative heat transfer*, Oxford: Academic press, (2013), pp. 498-529
- [27] Siegel, R., Howell, J.R., *Thermal Radiation Heat Transfer*, Published by Taylor & Francis, New York, USA, Fourth Edition, (2002), pp. 44-46
- [28] Atashafrooz, M. and Gandjalikhan Nassab, S. A., Numerical analysis of laminar forced convection recess flow with two inclined steps considering gas radiation effect, *Computer & Fluids*, 66(2012), pp. 167-176
- [29] Ozisik, M. N., Orlande, H. R. B., Inverse heat transfer, *Published by Taylor & Francis, New York, USA*, (2000), pp. 58-66
- [30] Bahraini, S., Gandjalikhan Nassab, S.A., Sarvari, S.M.H., Inverse Convection-Radiation Boundary Design Problem of Recess Flow with Different Conditions, *Iranian Journal of Science and Technology, Transactions of Mechanical Engineering*, 40 (2016),3, pp.215-222.
- [31] Touloukian, Y. S. and DeWitt, P. D., Thermophysical Properties of Matter - The TPRC Data Series. Volume 7. Thermal Radiative Properties - Metallic Elements and Alloys,(1970)

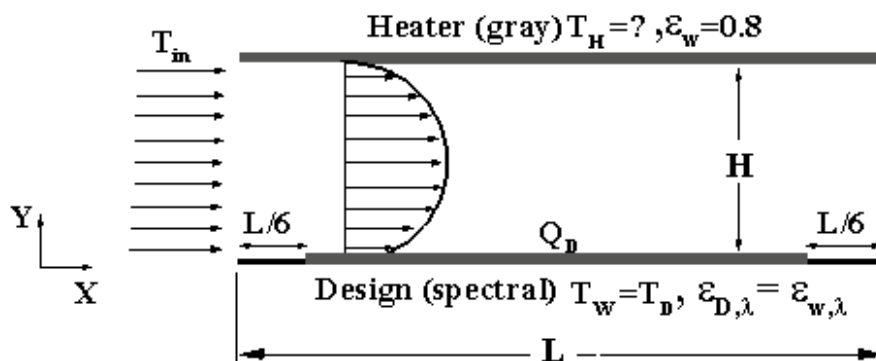


**Figure 1. Problem geometry**



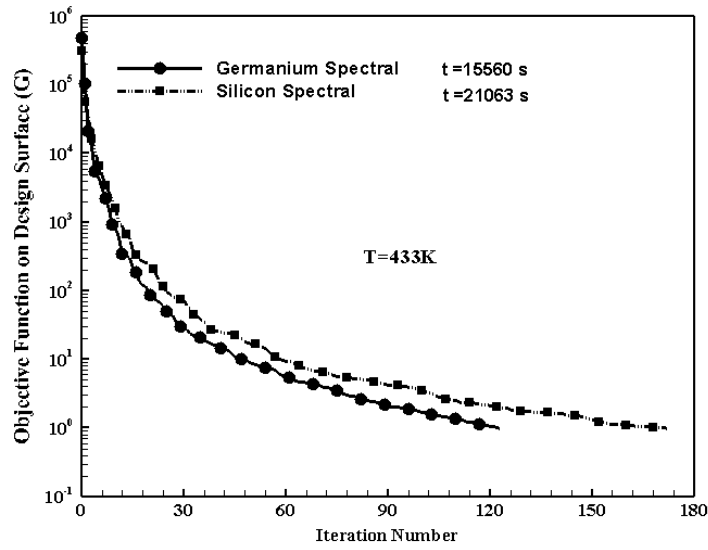


**Figure 2. Variation of objective function on design surface with iteration number**

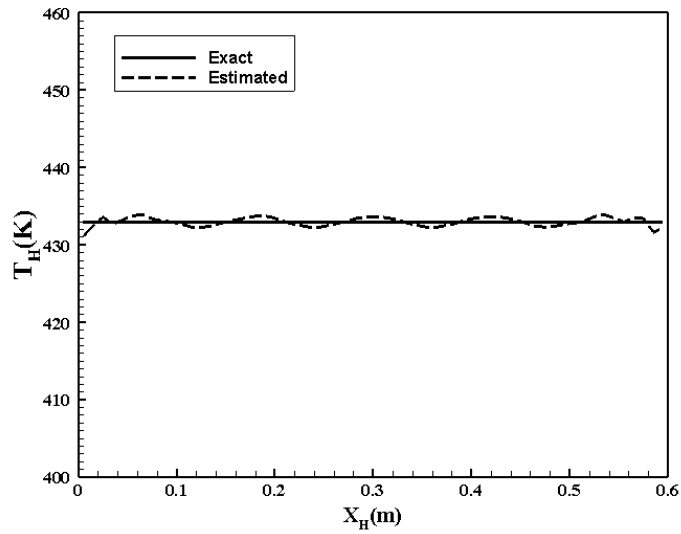


**Figure 3. Comparison of estimated and exact temperature distribution over the heater surface(validation of the inverse problem)**

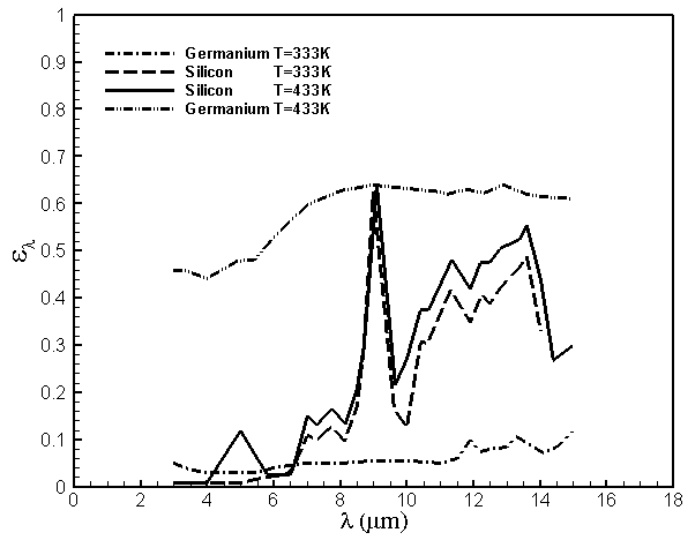


Figure 4. Normal spectral emissivities of Silicon and Germanium at different temperatures [31].

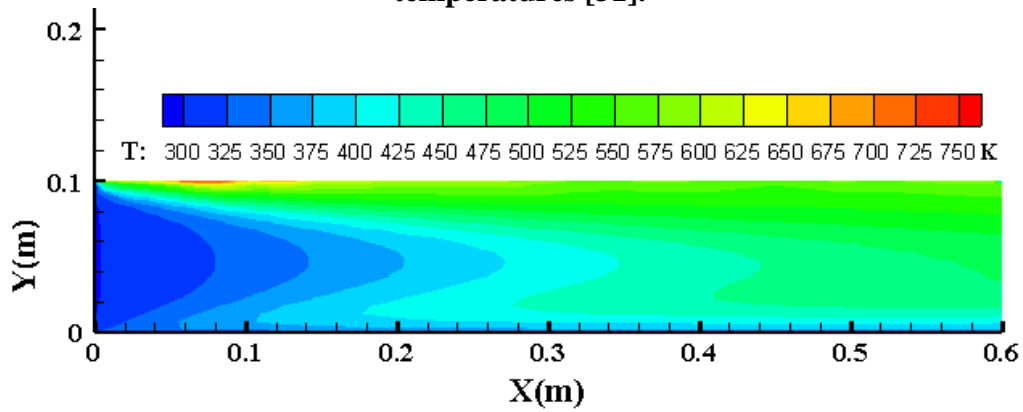


Figure 5. Temperature field in duct flow

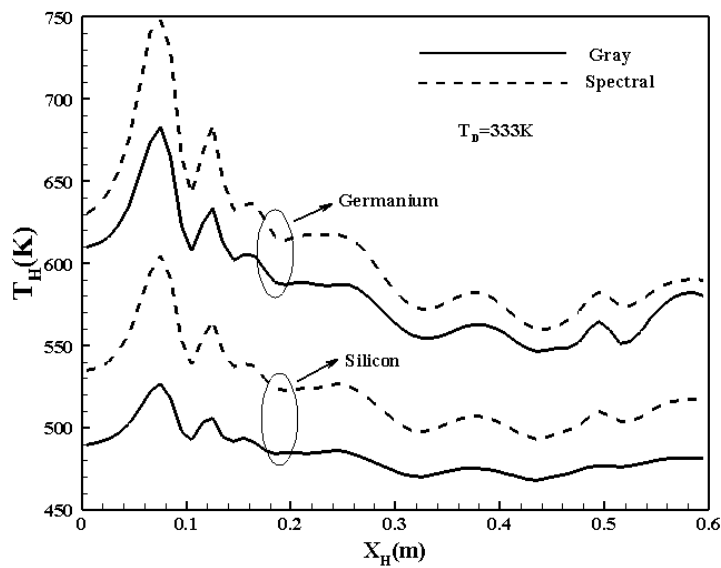
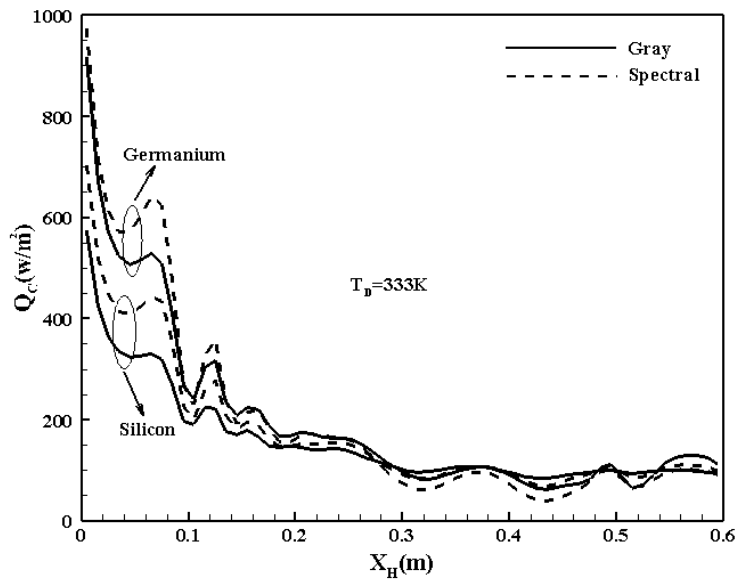
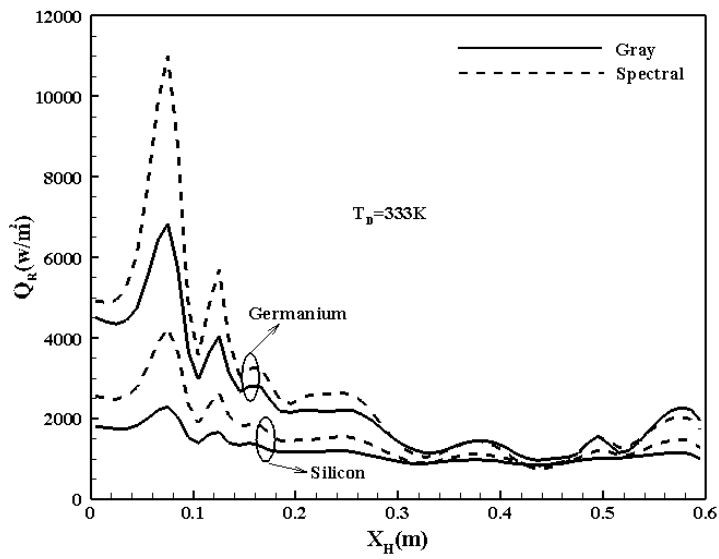


Figure 6. Temperature distribution over the heater surface



**a) Convective heat flux distribution**



**b) Radiative heat flux distribution**

**Figure 7. Distributions of convective and radiative heat flux over the heater surface**

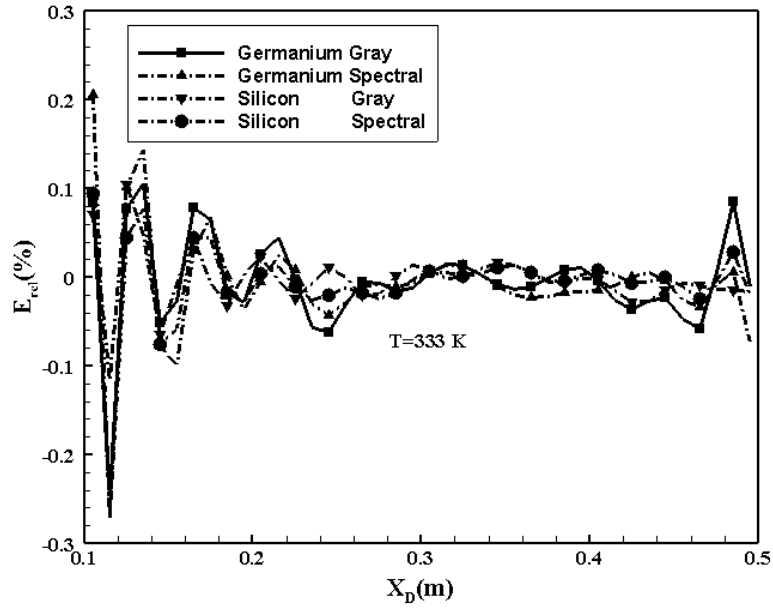


Figure 8. Relative error distribution over the design surface

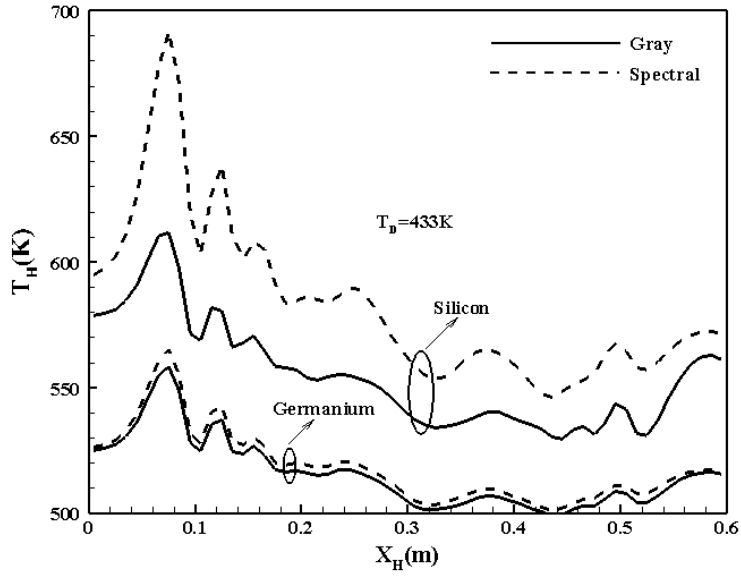


Figure 9. Temperature distribution over the heater surface

**Table 1. The band emissivities,  $\varepsilon_{\lambda,m}$  and the corresponding values of  $\Delta F_m$  for Germanium.**

m	1	2	3	4	5	6	7	8	9	10	11	12
$\lambda_{m-1} \rightarrow \lambda_m$	0-3.5	3.5-4	4-4.5	4.5-5	5.5-6	6-6.5	6.6-7	7-7.5	7.7-8	8-8.5	8.5-9	9-9.5
$\varepsilon_{\lambda,m}$	0.046	0.044	0.032	0.030	0.030	0.036	0.042	0.048	0.050	0.050	0.0541	0.054
$\Delta F_m \times 10^3$	0.32	1.3	3.6	7.5	12.4	17.9	23.2	27.9	31.8	34.6	36.5	37.5

m	13	14	15	16	17	18	19	20	21	22	23	24
$\lambda_{m-1} \rightarrow \lambda_m$	9.5-10	10-105	10.5-11	11-11.5	11.5-12	12-12.5	12.5-13	13-13.5	13.5-14	14-14.5	14.5-15	15-∞
$\varepsilon_{\lambda,m}$	0.055	0.055	0.053	0.051	0.056	0.086	0.078	0.083	0.099	0.084	0.079	0.106
$\Delta F_m \times 10^3$	37.4	36.6	35.5	34.2	32.6	31.1	29.4	27.8	26.2	24.6	23.1	388.7

**Table 2. Values of parameters**

<b>parameter</b>	<b>Value</b>	<b>Unit</b>
$\varepsilon_w$	<b>0.8</b>	-
$T_D$	<b>333, 433</b>	<b>K</b>
$Q_D$	<b>-500</b>	$W / m^2$
$\sigma_a$	<b>1</b>	$m^{-1}$
$\sigma_s$	<b>1</b>	$m^{-1}$
$T_{in}$	<b>298</b>	<b>K</b>